MOLECULAR AND CELLULAR BIOLOGY, Nov. 2005, p. 9221–9231 Vol. 25, No. 21
0270-7306/05/$08.00+0 doi:10.1128/MCB.25.21.9221–9231.2005

Novel *PMS1* Alleles Preferentially Affect the Repair of Primer Strand Loops during DNA Replication

Naz Erdeniz,[1] Sandra Dudley,[1] Regan Gealy,[2] Sue Jinks-Robertson,[2] and R. Michael Liskay[1]*

Molecular and Medical Genetics, Oregon Health and Science University, L103, 3181 SW Sam Jackson Park Road, Portland, Oregon 97239,[1] and Department of Biology, Emory University, 1510 Clifton Rd., Atlanta, Georgia 30322[2]

Received 14 March 2005/Returned for modification 11 April 2005/Accepted 21 July 2005

Null mutations in DNA mismatch repair (MMR) genes elevate both base substitutions and insertions/deletions in simple sequence repeats. Data suggest that during replication of simple repeat sequences, polymerase slippage can generate single-strand loops on either the primer or template strand that are subsequently processed by the MMR machinery to prevent insertions and deletions, respectively. In the budding yeast *Saccharomyces cerevisiae* and mammalian cells, MMR appears to be more efficient at repairing mispairs comprised of loops on the template strand compared to loops on the primer strand. We identified two novel yeast *pms1* alleles, *pms1-G882E* and *pms1-H888R*, which confer a strong defect in the repair of "primer strand" loops, while maintaining efficient repair of "template strand" loops. Furthermore, these alleles appear to affect equally the repair of 1-nucleotide primer strand loops during both leading- and lagging-strand replication. Interestingly, both *pms1* mutants are proficient in the repair of 1-nucleotide loop mispairs in heteroduplex DNA generated during meiotic recombination. Our results suggest that the inherent inefficiency of primer strand loop repair is not simply a mismatch recognition problem but also involves Pms1 and other proteins that are presumed to function downstream of mismatch recognition, such as Mlh1. In addition, the findings reinforce the current view that during mutation avoidance, MMR is associated with the replication apparatus.

DNA mismatch repair (MMR) contributes to genomic integrity by repairing mismatches generated during replication, by chemical damage, and as "heteroduplex" intermediates during recombination (7, 28, 31, 35, 44). In addition, the MMR system in higher eukaryotes plays a role in response to DNA damage (3, 6, 7, 62). Inherited MMR defects lead to a mutator phenotype, which in humans and mice is associated with increased cancer susceptibility (5, 7, 13, 16, 38, 50). The MMR system of *Escherichia coli* has been reconstituted in vitro with purified proteins, including the dedicated proteins MutS, MutL, and MutH (44, 56). The MutS protein, a homodimer, first binds the mispair, followed by recruitment of MutL, the endonuclease MutH, the UvrD helicase, four exonucleases, DNA polymerase, and ligase. Together with transient Dam-mediated hemimethylation, these proteins impose strand specificity that leads to specific repair of the newly replicated strand (10, 25, 26, 43, 44, 74).

In the budding yeast *Saccharomyces cerevisiae*, six MutS homologues (Msh proteins Msh1 to Msh6) and four MutL homologues (Mlh proteins, Mlh1 to Mlh3, and Pms1) function in various MMR transactions (7, 28, 31, 35). Unlike *E. coli*, the MutS and MutL activities of budding yeast and mammals are each comprised of heterodimers. Mismatches in nuclear DNA replication intermediates are recognized by the Msh2/Msh6 and Msh2/Msh3 heterodimers, which have partial functional overlap (7, 35, 42). Msh2/Msh6 operates in the repair of base-base mispairs and 1-nucleotide "insertion/deletion" loops (28, 32, 41), while Msh2/Msh3 functions in the repair of 1- to 4-nucleotide insertion/deletion loops (28, 32, 41). Similarly for the MutL homologs, Mlh1 forms heterodimers with Pms1, Mlh2, or Mlh3 (19, 28, 30, 49, 72). Genetic studies indicate that the Mlh1/Pms1 heterodimer is the primary MutL activity in MMR-mediated mutation avoidance, whereas the Mlh1/Mlh3 complex plays a minor role in Msh2/Msh3-dependent repair of insertion/deletion loops (19, 24, 30, 49, 53, 54). Current data suggest that initial recognition of the mismatch is by Msh2/Msh6 or Msh2/Msh3, possibly aided by PCNA, which is subsequently joined by Mlh1-Pms1 to form a higher order complex on DNA. This complex is thought to be responsible for directing the downstream and less well characterized MMR events, including strand discrimination, excision, and resynthesis (4, 7, 28, 35, 42).

Although the MutS and MutL proteins must interact during MMR-mediated mutation avoidance, the nature of these and other protein-protein interactions is not clear. Whereas *MLH1*, *PMS1*, and *MHS2* deletion mutations appear to result in a null, or near null, MMR state for mutation avoidance, specific *pms1* or *mlh1* mutant alleles might produce a novel mutator phenotype, for example, by differentially impacting interactions with Msh2/Msh3 or Msh2/Msh6. In turn, these types of alleles might provide additional insights into the function of the MutL homologs, including interactions with other MMR factors. Therefore, we have initiated genetic screens for mutations of *PMS1* or *MLH1* that result in mutational spectra different from the corresponding MMR-null strains. Here, we report the isolation of two novel *pms1* alleles, which in contrast to a *pms1*Δ strain preferentially elevate +1-bp frameshifts in mononucleotide runs, with little or no effect on −1-bp frameshifts. These *pms1* alleles are in close proximity, affecting residues near the end of the protein in a previously uncharacterized but highly conserved amino acid motif. Further analyses

* Corresponding author. Mailing address: Molecular and Medical Genetics, Oregon Health and Science University, L103, 3181 SW Sam Jackson Park Rd., Portland, OR 97239-3098. Phone: (503) 494-3475. Fax: (503) 494-6886. E-mail: liskaym@ohsu.edu.

TABLE 1. Strains used in this study

Strain	Genotype	Source or reference
W1558	*MAT*α *ade2-1 CAN1 his3-11,15 leu2-3,112 trp1-1 ura3-1 RAD5*	77
NEY190	W1558 *hom3-10*	This study
NEY186	NEY190 *pms1*::*TRP1*	This study
NEY398	NEY190 *pms1-G882E*	This study
NEY402	NEY190 *pms1-H888R*	This study
NEY524	*MAT*α *ade2-1 CAN1 his1-7 hom3-10 leu2-3,112 trp1-1 ura3-1 RAD5; HIS3 his1-7* derivative of NEY190	This study
NEY442	NEY524 *pms1*::*TRP1*	This study
NEY510	NEY524 *pms1-G882E*	This study
NEY506	NEY524 *pms1-H888R*	This study
NEY570	*MAT***a** *ade2-1 CAN1 his7-2 hom3-10 leu2-3,112 trp1-1 ura3-1 RAD5; HIS3 his7-2* derivative of NEY190	This study
NEY662	NEY570 *pms1*::*TRP1*	This study
NEY578	NEY570 *pms1-G882E*	This study
NEY574	NEY570 *pms1-H888R*	This study
NEY1106	NEY570 *msh2*::*LEU2*	This study
NEY1100	NEY570 *pms1*::*TRP1 msh2*::*LEU2*	This study
NEY1110	NEY570 *pms1-G882E msh2*::*LEU2*	This study
NEY1126	NEY570 *pms1-H888R msh2*::*LEU2*	This study
NEY815	NEY570 *pol2-C1089Y*	This study
NEY819	NEY570 *pms1*::*TRP1 pol2-C1089Y*	This study
NEY823	NEY570 *pms1-G882E pol2-C1089Y*	This study
NEY827	NEY570 *pms1-H888R pol2-C1089Y*	This study
SJR1973	*MAT***a** *ade2-101*$_{oc}$ *his4*Δ::*LYS2R-10C lys2*Δ::*hyg trp1*Δ *ura3-52*	This study
NEY702	SJR1973 *pms1*::*URA3*	This study
NEY742	SJR1973 *pms1-G882E*	This study
NEY744	SJR1973 *pms1-H888R*	This study
NEY1084	SJR1973 *ogg1*::*TRP1*	This study
NEY1090	SJR1973 *pms1*::*URA3 ogg1*::*TRP1*	This study
NEY1092	SJR1973 *pms1-G882E ogg1*::*TRP1*	This study
NEY1094	SJR1973 *pms1-H888R ogg1*::*TRP1*	This study
SJR1977	*MAT***a** *ade2-101*$_{oc}$ *his4*Δ::*LYS2F-10C lys2*Δ::*hyg trp1*Δ *ura3-52*	This study
NEY706	SJR1977 *pms1*::*URA3*	This study
NEY747	SJR1977 *pms1-G882E*	This study
NEY749	SJR1977 *pms1-H888R*	This study
NEY1086	SJR1977 *ogg1*::*TRP1*	This study
NEY1088	SJR1977 *pms1*::*URA3 ogg1*::*TRP1*	This study
NEY1096	SJR1977 *pms1-G882E ogg1*::*TRP1*	This study
NEY1098	SJR1977 *pms1-H888R ogg1*::*TRP1*	This study
AS4	*MAT*α *trp1 arg4 tyr7 ade6 ura3*	61
NEY630	AS4 *pms1*::*URA3*	This study
NEY673	AS4 *pms1-G882E*	This study
NEY669	AS4 *pms1-H888R*	This study
PD24	*MAT***a** *leu2 ade6 ura3 his4-713*	11
NEY714	PD24 *pms1*::*URA3*	This study
NEY738	PD24 *pms1-G882E*	This study
NEY726	PD24 *pms1-H888R*	This study

suggest that these *pms1* alleles do not differentially impact MMR during leading- versus lagging-strand replication but, rather, fail to efficiently repair single nucleotide loops arising on the primer strand. The results presented here reinforce the current view that MMR is associated with the replication apparatus.

MATERIALS AND METHODS

Media and growth conditions. All media were prepared as described (58) except that synthetic medium contained increased leucine (60 mg/liter). Growth and sporulation were at 30°C and at 18°C, respectively. Sporulation of diploid cells and tetrad dissections were performed as previously described (15, 73).

Strain constructions. Yeast strains used for assaying *CAN1* forward mutations or *his1-7*, *his7-2*, and *hom3-10* reversion are derivatives of a *RAD5 CAN1* W303-1B strain (65) (Table 1). The *hom3-10* allele was introduced at the *HOM3* locus by a two-step recombination procedure using the plasmid pK8 linearized with SpeI (41). Presence of the *hom3-10* allele was verified by the inability of the strain to grow on medium lacking threonine. The *his1-7* (71) and *his7-2* (57) alleles were introduced by a cloning-free, PCR-based allele replacement approach (14). The sequences of primers are the following (with uppercase letter sequences denoting the adaptamer sequences and lowercase letters denoting *HIS1* or *HIS7* sequences): *his1-7* Adap A (5′-AATTCCAGCTGACCACCATG AAattgagagaaaaacgaaggg-3′) and *his1-7* Adap B (5′-GATCCCCGGGAATTG CCATGctgacaaatatgctacgaag-3′) for *his1-7*, and *his7-2* Adap A (5′-AATTCCA GCTGACCACCATGgcgtcgggctacaagcgc-3′) and *his7-2* Adap B (5′-GATCCC CGGGAATTGCCATGctgtgccaactgaacaggc-3′) for *his7-2*. Introduction of the mutant allele was verified by the inability of the strain to grow on medium lacking histidine and confirmed by sequencing analysis.

Strains containing 10C runs were constructed using a derivative of YPH45 (*MAT***a** *ura3-52 ade2-101*$_{oc}$ *trp1*Δ*1*) in which the open reading frame of *LYS2* was replaced with a hygromycin resistance cassette (*lys2*Δ::*hyg*) by transformation with a PCR fragment derived from hphMX4 (20). A wild-type *LYS2* gene was then inserted at the *HIS4* locus on chromosome III by transformation with a PCR fragment amplified from pDP6 (17) using primers with terminal homology to the *HIS4* locus. The primer pair Lys2FHis4F2 (5′-ACTTGGTTGAACAAT TGAATGTACCAAAGGAGCGTGTTGTTGTGGAAGAGAACGGTGTTTa gaggcatcgcacagttttagc-3′; base pairs complementary to *HIS4* sequences are in uppercase while those complementary to *LYS2* are in lowercase) and Lys2RHis4R (5′- GTTCGGTTTCCAAGTTAGAAATAATCTACTGGAAAT CCTTTGGGATCAACCCAAGCTTACccgaaaagaagctaagtctt-3′) were used to

generate a fragment for inserting *LYS2* at *HIS4* in the forward orientation (*his4*Δ::*LYS2F*), with *LYS2* transcribed in the same direction as *HIS4*. The primer pair Lys2Fhis4R2 (5′-GTTCGGTTTCCAAGTTAGAAATAATCTACT GGAAATCCTTTGGGATCAACCCAAGCTTActagaggcatcgcacagttttagc-3′) and Lys2RHis4F (5′-ACTTGGTTGAACAATTGAATGTACCAAAGGAGCG TGTTGTTGTGGAAGAGAACGGTGTTTccgaaaagaagctaagtctt-3′) were used to generate a fragment for inserting *LYS2* at *HIS4* in the reverse orientation (*his4*Δ::*LYS2R*), with *LYS2* transcription opposing that of *HIS4*. In strains with the *his4*Δ::*LYS2F* allele, transcription and replication fork movement proceed in the same direction; in strains with the *his4*Δ::*LYS2R* allele, the direction of transcription opposes that of replication fork movement.

Mononucleotide run of 10C was inserted into the coding strand of the *his4*Δ::*LYS2* alleles using the delitto perfetto method (63). First, the CORE cassette containing *URA3* and *Kan* was amplified with the primer pair CORE406Lys2F (5′-CGAGCTAGCTGAAAAATTCAAAGTTGCCAAGATC TGGAAAGGACCCCTCgagctcgttttcgacactgg-3′; uppercase letters denote the *LYS2* sequence and lowercase letters denote CORE cassette sequence) and CORE406Lys2R (5′-CTCGTCTAATTTGAAATCTTGGTTTTCCAAAAAG GCCAAACGGAACAACTtccttaccattaagttgatc-3′), with the CORE cassette inserted after base pair position 406 relative to the *LYS2* start codon. Following transformation with the amplified fragment, Ura^+, geneticin-resistant transformants were selected and screened for a Lys^- phenotype. The CORE cassette within *LYS2* was then replaced with a 240-bp *LYS2-10C* fragment amplified from SJR1354 (21). Lys^+ transformants were selected and screened for loss of CORE sequences (Ura^-, geneticin-sensitive phenotype). The presence of the 10C run was confirmed by sequence analysis. Runs are named according to the nucleotides on the coding strand; a *LYS2-10C* allele thus has a 10C run on the coding strand and the complementary 10G run on the noncoding strand.

PMS1 and *OGG1* disruptions were constructed in relevant haploid strains by a PCR-based gene disruption method (2) utilizing *TRP1* and *URA3* for *PMS1* and *TRP1* for *OGG1* as selective markers and the following primer pairs (uppercase letters indicate sequences complementary to *PMS1* or *OGG1* sequences and lowercase letters denote selective marker sequences): *PMS1*-L1 (5′-CGAA AAGAAAAGACGCGTCTCTCTTAATAATCATTATGCGATAAAgagcagatt gtactgag-3′) and *PMS1*-L2 (5′-ATAATGTATTTGTTAATTATATAATGAAT GAATATCAAAGCTAGAtgtgcggtatttcacacc-3′; *OGG1*-L1 (5′-TTTGAAGCG TCCTGATTCATAATTGCGATTTTATTTATCAACCAGgagcagattgtactgag-3′) and *OGG1*-L2 (5′-TTCGGTCGCGTGCTTTTATCGTGGTATTTACTAT GACTTTTTAAGtgtgcggtatttcacacc-3′). Each disruption was confirmed by PCR.

The alleles *pms1-G882E* and *pms1-H888R* were each integrated into the genome by the cloning-free, PCR-based allele integration approach described above (14). Primers used to amplify either *pms1-G882E* or *pms1-H888R* are the following (with uppercase letters denoting the adaptamer sequence and lowercase letters for PMS1 sequence): *PMS1* C-term Adap A (5′-aattccagctgaccacca tgGAAGACGGTGGGTTACGAAG-3′) and *PMS1* C-term Adap B (5′-gatcccc gggaattgccatgCAAGCATCTTCAATGCACGAG-3′). The fusion fragments were cotransformed into relevant strains and Ura^+ transformants were selected. Subsequent retention of a single copy of the mutant *pms1* allele after 5-fluoroorotic acid selection was verified by PCR and sequencing using primers *PMS1* C-term Adap A and *PMS1* C-term Adap B.

pol2-C1089Y was introduced by a two-step allele replacement method (55). AgeI linearized p173-rsa (33) was transformed into cells, followed by selection on medium lacking uracil. Ura^+ transformants were purified and grown in YPD medium (containing yeast extract, peptone, and glucose) and streaked to 5-fluoroorotic acid plates to select for Ura^- colonies, which were screened for the *pol2-C1089Y* mutation by PCR and diagnostic digestion with RsaI.

Plasmid constructions. Plasmid pRS414-*PMS1* was constructed by inserting a 4-kb chromosomal BglII/SalI fragment that contains the 2,715-bp *PMS1* open reading frame (ORF) into BglII/SalI-digested pRS416 (*URA3-CEN* vector [60]). Plasmids used in two-hybrid assays were constructed by inserting coding sequences of *MLH1* and *PMS1* into pBTM116 and pGAD424, which contain the LexA DNA-binding domain and Gal4 activation domain, respectively (49). The *pms1-G882E* and *pms1-H888R* alleles were introduced into the pGAD424-*PMS1* plasmid by gap repair (40, 48). Three independent plasmids from each transformation were sequenced to verify the *pms1-G882E* and *pms1-H888R* mutations.

Construction of a randomly mutagenized *PMS1* library. PCR mutagenesis of the *PMS1* ORF was carried out in two separate reactions (75). The primer pair *PMS1*-MluI (5′-GCACAGATTAATACCGATTC-3′) and *PMS1*-BsaBI (5′-GC GTAGAGTATTCCACTGGC-3′) and the pair *PMS1*-ClaIF (5′-CGCAGAGA TTGAGCCAGTTG-3′) and *PMS1*-ClaIRev (5′-GACGATTGAAGGAGACG CTAG-3′) were used to mutagenize the first approximately one-third (fragment I) and the last approximately one-third (fragment II) of the *PMS1* ORF, respectively. The PCR mixture contained the following components: 10 mM Tris-HCl, 1.5 mM $MgCl_2$, 50 mM KCl (pH 8.3), 0.25 mM $MnCl_2$, a 200 μM concentration of each deoxynucleoside triphosphate, a 1 μM concentration of each primer, 5 U of *Taq* DNA polymerase, and 10 ng of plasmid pRS414-*PMS1*. The PCR conditions were 5 min at 94°C and 40 cycles of 15 s at 94°C, 15 s at 50°C, and 1 min at 72°C, followed by 10 min at 72°C.

The PCR-mutagenized fragments I and II were gel purified and cotransformed individually into yeast strain NEY186 with pRS416-*PMS1* linearized with MluI/BsaBI or ClaI, respectively. Transformants were selected on synthetic complete medium lacking uracil. In vivo homologous gap repair recombination between the PCR fragments and the vector DNA produced a library of mutagenized *pms1* alleles on a *CEN* plasmid. Control transformations with only the gapped vector indicated >95% efficiency in gap repair. A total of 2,000 transformants of each mutagenized fragment were patched onto medium lacking uracil. After 2 days, the patches were replica plated onto synthetic complete medium lacking uracil and arginine but containing canavanine and onto medium lacking uracil and threonine to score mutation at *CAN1* and *hom3-10*, respectively. Plasmid DNAs from two transformants that consistently exhibited a mutator phenotype on canavanine, but not in the *hom3-10* reversion assay, were used to retransform NEY186.

Rate measurements and statistical analyses. The method of the median was used to calculate the mutation rate (37). Data from at least 20 independent cultures (typically four cultures from each of five independent isolates) were used for each rate determination. In all cases, different isolates behaved the same as evidenced by side-by-side comparisons. Briefly, purified colonies were grown in liquid yeast extract-peptone-dextrose medium to saturation. Appropriate dilutions were plated onto complete synthetic medium to determine the viability of the cells. Medium lacking histidine was used to select His^+ prototrophs; medium lacking threonine was used to select revertants of *hom3-10*; medium lacking arginine but containing canavanine was used to select *can1* mutants; and medium containing alpha amino-adipic acid (8) was used to select Lys^- mutants. Colonies were counted 3 to 5 days after selection plating. Statistical analyses were performed using Prism 3.0 software (GraphPad Software Inc.). The efficiencies of mismatch correction (repair efficiencies) were determined by comparing the rates of instability at the *LYS2-10C* locus in *pms1*Δ strains to the rates observed in wild-type, *pms1-G882E*, and *pms1-H888R* strains (59). If we denote the rate of instability as R_{wt}, $R_{pms1\Delta}$, $R_{pms1\text{-}G882E}$, and $R_{pms1\text{-}H888R}$ in wild-type, *pms1*Δ, *pms1-G882E*, and *pms1-H888R* strains, respectively, then the repair efficiency is calculated by substracting the mutation rate after repair (R_{wt}, $R_{pms1\text{-}G882E}$, or $R_{pms1\text{-}H888R}$) from mutation rate before repair ($R_{pms1\Delta}$) and then dividing this difference by the mutation rate before repair ($R_{pms1\Delta}$).

Two-hybrid analysis. Protein-protein interactions were assayed by the two-hybrid method as previously described (49).

Sequence analysis of mutants. Independent isolates for sequence analysis were obtained by streaking individual colonies onto appropriate selective medium. The relevant gene regions were amplified from the yeast genome by "colony PCR" (39). PCR products were sequenced using the following primers: for *CAN1*, *CAN1* For (5′-CTTAACTCCTGTAAAAAC-3′), *CAN1* Seq1 (5′-C ATTGGCCGCACCAAATGC-3′), *CAN1* Seq2 (5′-TTCATCCCTGTTACATC C-3′), *CAN1* Seq3 (5′-CCAAATGCAGCAGTAACG-3′), and *CAN1* Rev (5′-G AAATGGCGTGGGAATGT-3′); for *LYS2*, *LYS2* 5′ (5′-GCTACATATTCGT TACAGC-3′) and *LYS2* 3′ (5′-GGTCCGCAACAATGGTTACTC-3′); and for *his1-7*, *HIS1* For (5′-CTCCTATTAACGGTTTGAATC-3′) and *HIS1* Rev (5′-GAATAAGATAGAACTCTATC-3′).

RESULTS

To understand better the role of the Mlh1/Pms1 (MutLα) heterodimer in MMR, we set out to identify alleles of *PMS1* that differentially impact MMR-mediated mutation avoidance. Thus, we mutagenized the most conserved regions of the yeast *PMS1* ORF and screened for alleles that resulted in a mutator phenotype different from that seen in a *pms1*Δ strain. A library of randomly mutagenized *PMS1* genes in a *CEN* vector was screened initially in a *pms1*Δ strain using two mutation assays: reversion of *hom3-10* and forward mutation to canavanine resistance at *CAN1*, which report −1-bp frameshifts in a 7A/7T run and multiple types of mutations, respectively (Fig. 1a and b). Previous work demonstrated that in a *pms1*Δ strain, reversion of *hom3-10* was increased approximately 1,000-fold while

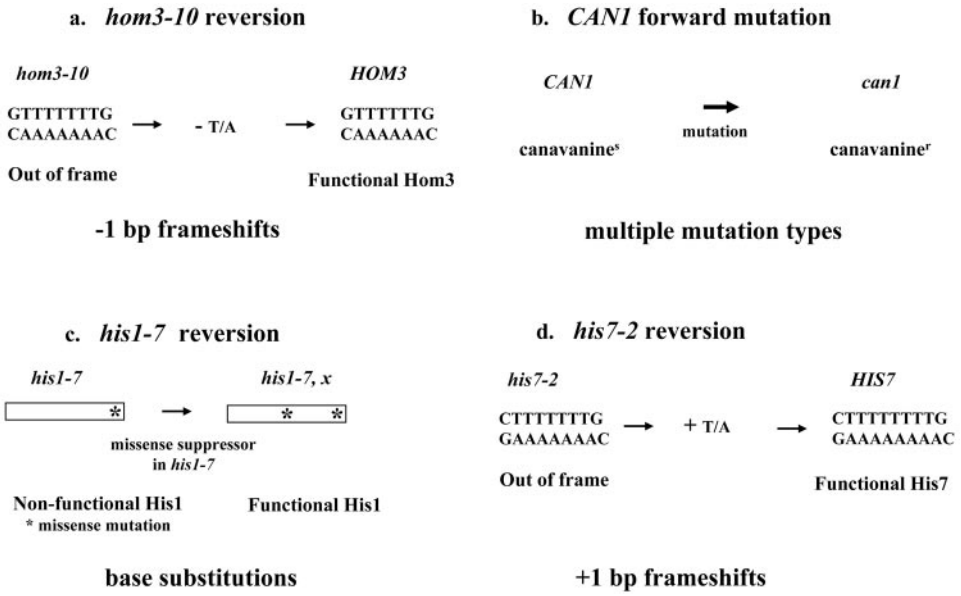

FIG. 1. Schematic of four mutator assays. (a) *hom3-10* reversion assay measures −1-bp frameshifts in a stretch of 7A/7T bp. (b) *CAN1* forward mutation assay detects multiple types of mutations. (c) *his1-798* (*his1-7*) reversion assay measures intragenic missense suppressor mutations near the 3′ end of *HIS1*. (d) *his7-2* reversion assay reports +1-bp frameshifts in a run of 7A/7T bp.

forward mutation at the *CAN1* locus was increased 30-fold, with more than 60% of the *can1* mutations being −1-bp frameshifts in short mononucleotide runs (67). In a *pms1*Δ strain, elevated mutation levels at *hom3-10* and *CAN1* can be detected by an increased number of papillae on the appropriate selective media (Fig. 2a). Whereas most mutator strains increased papillation in both assays, two exceptional mutants consistently conferred a strong increase in the number of *can1*

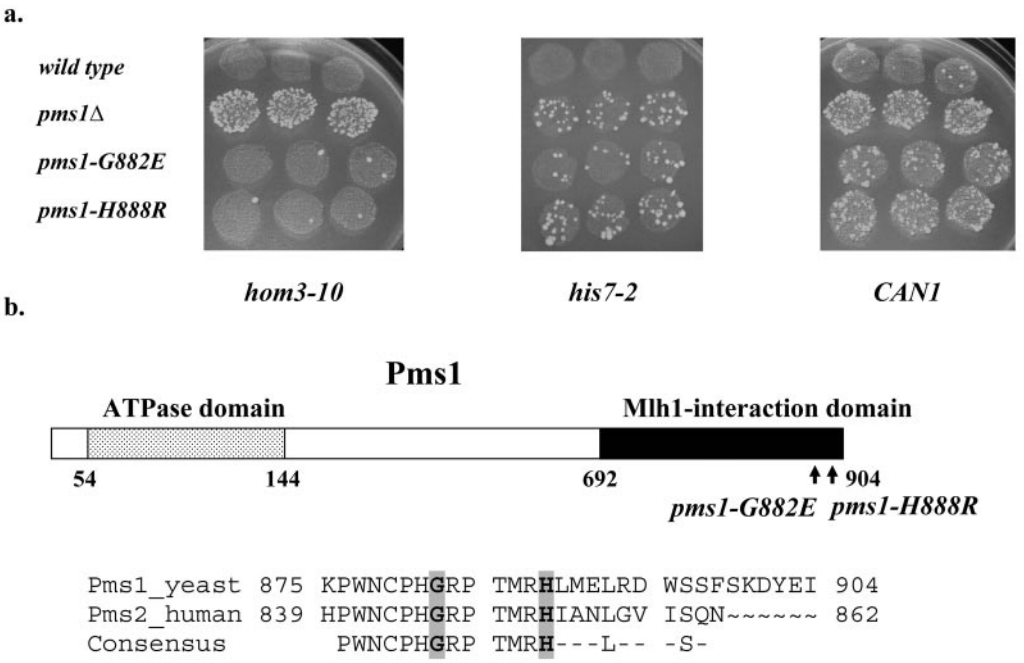

FIG. 2. (a) Papillation phenotypes of the wild-type, *pms1*Δ, *pms1-G882E*, and *pms1-H888R* strains. The relative mutator effects at *hom3-10*, *his7-2*, and *CAN1* alleles in wild-type, *pms1*Δ, *pms1-G882E*, and *pms1-H888R* strains were detected initially by monitoring reversion at *hom3-10* and *his7-2* and the forward mutation of *CAN1* alleles individually by replica plating patches of cells onto appropriate selective media. (b) Pms1 domains and location of altered Pms1 residues. The ATPase domain (residues 54 to 144) and the Mlh1-interacting domain (residues 692 to 904) are indicated by dotted and black boxes, respectively. Also shown are the residues corresponding to the COOH termini of yeast and human homologs. The mutated residues, G882 and H888, are shaded gray. The 13-amino-acid domain, identical between yeast and human homologs, is depicted below the alignment of yeast and human homolog sequences. Numbers correspond to the amino acid position in the protein.

TABLE 2. Mlh1/Pms1 two-hybrid interactions

Strain	β-Galactosidase activity	Increase (fold)
pBT+pGAD-*PMS1*	0.18±0.05	1
pBT-*MLH1* + pGAD-*PMS1*	10.8 ±1.8	60
pBT-*MLH1* + pGAD-*pms1-G882E*	7.8 ±0.09	43
pBT-*MLH1* + pGAD-*pms1-H888R*	10.3 ±0.4	57

papillae but no detectable increase in reversion at *hom3-10* (Fig. 2a). We did not detect any candidates with the opposite phenotype. To address strain-specific effects, we tested the two *pms1* alleles on *CEN* plasmids in two additional strain backgrounds, GCY35 (45) and AMY125 (59), and observed similar results (data not shown). DNA sequencing analysis of these two unusual *pms1* alleles revealed in each strain the presence of a single mutation resulting in a change of glycine to glutamate at residue 882 (*pms1-G882E*) or histidine to arginine at residue 888 (*pms1-H888R*) (Fig. 2b).

Pms1-G882E and Pms1-H888R interact efficiently with Mlh1 and are expressed at wild-type levels. Because residues G882 and H888 both lie in the C-terminal region of Pms1, which is essential for interaction with Mlh1 (49), we tested the ability of the mutant proteins to interact with Mlh1 using a two-hybrid assay. As shown in Table 2, both mutant forms of Pms1 interacted efficiently with Mlh1. In addition, we determined the expression levels of Pms1-G882E and Pms1-H888R at the endogenous *PMS1* locus. No significant differences between the levels of FLAG-tagged Pms1-G882E, Pms1-H888R, or wild type Pms1 were observed using Western blot analysis (data not shown). Together, comparison of Pms1 protein levels and the two-hybrid assay suggest that the *pms1-G882E* and *pms1-H888R* alleles have little if any effect on protein stability or interaction with Mlh1.

Further analysis of the *pms1-G882E* and *pms1-H888R* mutator phenotype. To confirm the differential effects of *pms1-G882E* and *pms1-H888R* in the *hom3-10* and *CAN1* mutator assays, the plasmid-encoded alleles were introduced at the endogenous *PMS1* locus in wild-type strain NEY190. As shown in Table 3, both *pms1-G882E* and *pms1-H888R* strains displayed significantly elevated mutation rates at *CAN1*, although both alleles caused less of a mutator phenotype than seen in a *pms1*Δ strain (3-fold and 5-fold increases, respectively, versus a 17-fold increase in *pms1*Δ). In contrast, whereas *pms1*Δ resulted in a 1,100-fold increase in *hom3-10* reversion, the *pms1-G882E* and *pms1-H888R* strains displayed only 3- to 4-fold increases in *hom3-10* reversion relative to wild type (Table 3).

To gain additional insight into the MMR defects, we tested the *pms1-G882E* and *pms1-H888R* alleles using *his1-798* (*his1-7*) reversion, which reports intragenic missense suppressor mutations near the 3′ end of *HIS1* (Fig. 1) (71). First, the *his1-7* allele was integrated and characterized in wild-type and *pms1*Δ backgrounds. *pms1*Δ strains displayed a ninefold elevated *his1-7* reversion rate compared to the wild type (Table 3). As predicted (71), all 20 revertants from the *pms1*Δ strain were sequenced and found to be intragenic missense suppressors at *HIS1* locus (data not shown). The *pms1-G882E* strain did not display a significant increase in the base substitution rate. However, the *pms1-H888R* strain showed a small but significant threefold increase over the wild type in base substitutions (Table 3).

Next, we tested the *pms1* alleles using the *his7-2* reversion assay, which reports +1-bp frameshifts in a run of 7A/7T bp (Fig. 1). With the *his7-2* assay, the *pms1*Δ strain displayed a 172-fold increase in +1 frameshifts compared to a wild-type strain (Table 3). Strikingly, in contrast to their behavior with *hom3-10* reporter, both *pms1-G882E* and *pms1-H888R* were similar to *pms1*Δ with the *his7-2* reporter. The reversion rate for *his7-2* was elevated 56- and 153-fold in the *pms1-G882E* and *pms1-H888R* strains, respectively (Table 3).

Based on rate analyses with four mutator reporters (*CAN1*, *hom3-10*, *his1-7*, and *his7-2*), the *pms1-G882E* and *pms1-H888R* alleles both appeared to preferentially elevate +1-bp frameshifts in mononucleotide runs. To confirm this interpretation, 20 to 30 *can1* mutants from each strain were sequenced. Strikingly, in *pms1-G882E* and *pms1-H888R* strains, approximately 40% of the *can1* mutations were +1-bp frameshifts, whereas in wild-type and *pms1*Δ strains, this percentage was only 5% (Table 4).

Taken together, the most notable finding from the mutation analyses is that *pms1-G882E* and *pms1-H888R* alleles increase +1-bp frameshifts in mononucleotide repeats to an extent comparable to that associated with a *pms1*Δ allele, while having little or no effect on −1-bp frameshifts and no or little effect on base substitutions. The preferential increase in the +1-bp frameshifts is in contrast to *pms1*Δ or other MMR-null strains, which generally show a greater increase in −1-bp frameshifts in mononucleotide reporters (21). Our findings suggest that the *pms1-G882E* and *pms1-H888R* alleles are preferentially defective in repairing single-strand loops arising on the primer strand during DNA replication (Fig. 3).

***pms1-G882E* and *pms1-H888R* mutator effects are similar during leading- and lagging-strand synthesis.** The mutation data presented above suggest that the *pms1-G882E* and *pms1-*

TABLE 3. Mutation rates at *CAN1, his1-7, hom3-10* and *his7-2*

Strain	*CAN1*		*his1-7*		*hom3-10*		*his7-2*	
	Mutation rate (10^{-7})[a]	Increase (fold)[b]	Mutation rate (10^{-7})[a]	Increase (fold)[b]	Mutation rate (10^{-8})[a]	Increase (fold)[b]	Mutation rate (10^{-9})[a]	Increase (fold)[b]
PMS1	4.3 (3.4–5.2)	1	2.6 (1.1–4)	1	1.01 (0.13–2)	1	5.9 (3.8–8)	1
*pms1*Δ	71 (50–92)	17	23 (14–32)	9	1,170 (400–1947)	1,100	1020 (990–1,050)	172
pms1-G882E	13 (8.4–17)	3	4.4 (3.2–5.5)	1.7	4 (3.1–4.9)	3.7	329 (277–381)	56
pms1-H888R	20 (17–23)	4.7	8 (4.2–11.7)	3.1	3.6 (2.7–4.5)	3.4	903 (821–984)	153

[a] Values in parentheses are 95% confidence intervals.
[b] Increases are calculated relative to *PMS1*.

TABLE 4. Spectra of *can1* mutations

Strain	*CAN1* mutation rate (10^{-7})[a]	No. of base substitutions/ no. of mutants sequenced (fold increase)[b]	No. of frameshifts/no. of mutants sequenced (fold increase)[b]	
			−1 bp	+1 bp
PMS1	4.3 (3.4–5.2)	15/20 (1.0)	4/20 (1.0)	1/20 (1.0)
*pms1*Δ	71 (50–92)	13/27 (11)	13/27 (41)	1/27 (13)
pms1-G882E	13 (8.4–17)	14/30 (1.9)	4/30 (2.0)	12/30 (24)
pms1-H888R	20 (17–23)	15/30 (3.1)	2/30 (1.6)	13/30 (41)

[a] Values in parentheses are 95% confidence intervals.
[b] Increases are calculated relative to *PMS1*.

H888R alleles differentially affect the repair of +1-bp versus −1-bp frameshift intermediates, with a much greater defect in the repair of mispairs due to 1-nucleotide loops on the primer strand than 1-nucleotide loops on the template strand. However, because these data were derived using different genes at different positions in the yeast genome, the mutation pattern might instead reflect sequence effects (e.g., more efficient repair of extra A than of extra T) and/or differences in the repair of errors generated during leading- versus lagging-strand synthesis.

A more direct comparison of the repair efficiencies of +1 versus −1 frameshift intermediates requires the use of a single mutational target for both types of events. Therefore, we constructed strains with an in-frame 10C run on the coding strand of the *LYS2* gene (*LYS2-10C*). As shown previously, a 10N run is sufficiently long to insure that the majority of *lys2* forward mutations occur within the run (21, 29, 66). Whether a given sequence resides on the leading- or lagging-strand template during replication was controlled by positioning the *LYS2-10C* allele at the *HIS4* locus on chromosome III, which is replicated from *ARS306* >90% of the time (46, 76). We define the forward (*LYS2F*) orientation as that in which the transcriptional machinery and replication fork move in the same direction; in the reverse (*LYS2R*) orientation, they converge (Fig. 4). To change the location of a given run on the leading- versus lagging-strand template, we inverted the entire *LYS2-10C* gene. As illustrated in Fig. 4, the 10C run is on the lagging-strand template in strains containing the *LYS2F-10C* allele but on the leading-strand template in strains containing *LYS2R-10C*.

For each *LYS2-10C* allele, we determined the forward mutation rate and mutational spectrum in *PMS1*, *pms1*Δ, *pms1-G882E*, and *pms1-H888R* backgrounds (Table 5). In the wild type, the forward mutation rates for the *LYS2F-10C* and *LYS2R-10C* alleles were similar, and an approximately 10:1 bias for +1 events was observed, suggesting less efficient repair of +1 than of −1 frameshift intermediates. In spite of this apparent bias, however, it should be noted that the MMR efficiency for both +1 and −1 intermediates exceeded 95%. The forward mutation rates were elevated approximately 100-fold in the *pms1*Δ strains, with −1 events outnumbering +1 events approximately 2:1. These data from *PMS1* and *pms1*Δ backgrounds agree well with observations reported previously for strains containing the same *LYS2-10C* alleles at the *LYS2* locus in a different strain background (21). Although the forward *LYS2* mutation rates in the *pms1-G882E* and *pms1-*

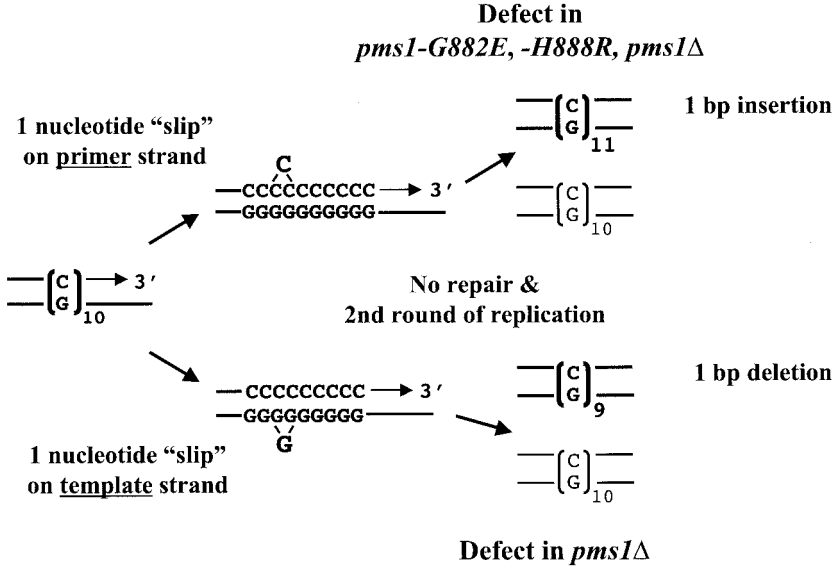

FIG. 3. DNA polymerase slippage model for instability in mononucleotide runs. Following a transient dissociation of the primer and template strand during DNA replication, the strands can reanneal in misaligned configuration, resulting either in a displaced single-strand loop on the primer (upper) or the template (lower) strand. If the resulting mismatches are not corrected before the next round of replication, the mispaired loops will give rise to unit size insertions or deletions, depending on whether the unpaired loop was in the primer or the template, respectively.

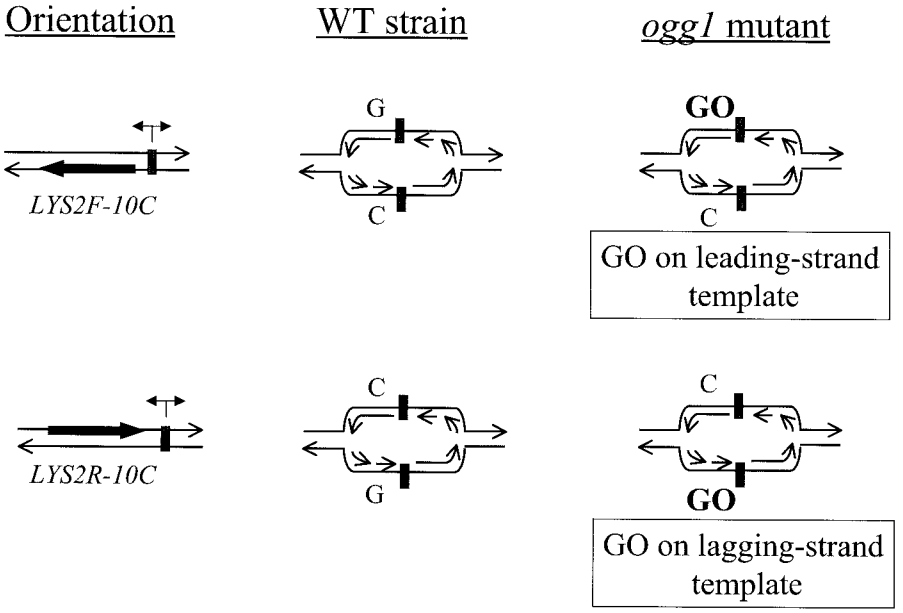

FIG. 4. Schematic representation of replication forks emerging from *ARS306*. The location of *ARS306* is depicted as a gray box. The coding (nontranscribed) *LYS2* strand is illustrated as a thick black arrow, whereas the bi-directional arrow above *ARS306* indicates the directionality of replication from *ARS306*. The forward (*LYS2F*) orientation is defined as that in which the transcriptional machinery and replication fork move in the same direction; in the reverse (*LYS2R*) orientation, they converge. The 10G run is on the leading-strand template whereas the 10C run is on the lagging-strand template in strains containing the *LYS2F-10C* allele. With the *LYS2R-10C*, the 10G run is on the lagging-strand template, and the 10C run is on the leading-strand template.

H888R strains were comparable to the *pms1*Δ strain rates, the distributions of +1 versus −1 events within the 10C/10G runs were not. There was a very strong bias for +1 events (39:1), which is the reverse of that seen in the *pms1*Δ strains, but very similar to the bias in the *PMS1* strains. The C/G runs of the *LYS2-10C* alleles thus behave similarly to the A/T runs of the *hom3-10* and *his7-2* alleles and support the conclusion that the primary MMR defect conferred by the *pms1-G882E* and *pms1-H888R* alleles is in the repair of primer strand loop mispairs (Fig. 3).

Although the above data demonstrate that the inefficiency in primer strand loop repair conferred by the *pms1-G882E* and *pms1-H888R* alleles is not sequence specific, the analysis did not address the possibility of differential effects during leading- versus lagging-strand synthesis. Addressing the leading/lagging issue requires knowledge of which strand the mutation originated on, which can be deduced using a strain deficient in *OGG1*, a glycosylase that specifically initiates repair of 8-oxo-7,8-dihydroguanine (GO) lesions (70), which can base pair efficiently with adenine as well as cytosine. In an *ogg1* mutant, the resulting increase in GC to TA transversions reflects specifically G-A rather than C-T mispairings, thus assigning the strand on which the original mispair occurred (51). We reasoned that if the presence of a GO lesion in the template can stimulate DNA polymerase slippage, we should observe elevated frameshifts within the 10C/10G runs of the *LYS-10C* alleles in *ogg1* mutants. Using the same reasoning as applied to the transversions of GC to TA in *ogg1* mutants, we could assign a strandedness to the underlying slippage events because the initiating GO lesions would always be on the template strand.

TABLE 5. Forward mutation in *LYS2-10C* strains

Strain	10G lagging-strand template (*LYS2R-10C*)				10G leading-strand template (*LYS2F-10C*)			
	Rate (10^{-6})[a]	Increase (fold)[b]	No. of frameshifts[c]		Rate (10^{-6})[a]	Increase (fold)[b]	No. of frameshifts[c]	
			−1 bp	+1 bp			−1 bp	+1 bp
PMS1 OGG1	9.5 (7.3–11.6)	1	1/10	9/10	19.2 (14–23)	1	1/10	8/10
*pms1*Δ	1934 (886–2,981)	203	17/20	2/20	4,524 (1,797–7,251)	235	12/19	7/19
pms1-G882E	302 (153–451)	32	0/20	20/20	1,316 (600–2,032)	68	1/19	18/19
pms1-H888R	693 (350–1,037)	73	0/20	20/20	1,651 (811–2,490)	86	0/20	19/20
*ogg1*Δ	91 (12–170)	9.5	0/12	7/12	96.5 (70–123)	5	0/12	8/12
*pms1*Δ *ogg1*Δ	11,950 (4,310–28,220)	1,258	8/13	5/13	16,570 (7,190–25,940)	863	8/13	4/13
*pms1-G882E ogg1*Δ	5,587 (1,770–9,390)	588	1/13	11/13	20,470 (14,360–26,570)	1,066	0/13	13/13
*pms1-H888R ogg1*Δ	8,420 (5,800–11,040)	886	0/13	11/13	29,100 (8,010–50,180)	1,516	0/13	11/13

[a] Values in parentheses are 95% confidence intervals.
[b] Increases are calculated relative to *PMS1*.
[c] Number/total number of mutants sequenced.

TABLE 6. Genetic interactions between *pms1* alleles and *msh2*Δ, *pol2-C1089Y*

Strain	*CAN1*		*his7-2*	
	Mutation rate (10^{-7})[a]	Increase (fold)[b]	Reversion rate (10^{-9})[a]	Increase (fold)[b]
PMS1 MSH2 POL2	4.3 (3.4–5.2)	1	5.9 (3.8–8)	1
*pms1*Δ	71 (50–92)	17	1,020 (990–1,050)	172
pms1-G882E	13 (8.4–17)	3	329 (277–381)	56
pms1-H888R	21 (17–24)	4.7	903 (821–984)	153
*msh2*Δ	66.1 (49–83)	15	1,450 (1,160–1,740)	246
*msh2*Δ *pms1*Δ	51 (33–69)	11.8	1,260 (910–1,600)	214
*msh2*Δ *pms1-G882E*	54 (32–75)	12.6	1,330 (520–2,130)	225
*msh2*Δ *pms1-H888R*	61.7 (26–98)	14.3	1,350 (1,200–1,490)	229
pol2-C1089Y	16 (11–21)	3.7	290 (30–551)	49
*pms1*Δ *pol2-C1089Y*	890 (454–1,300)	206	32,260 (7,000–57,530)	5,468
pms1-G882E pol2-C1089Y	372 (248–495)	86	26,000 (8,800–43,200)	4,406
pms1-H888R pol2-C1089Y	356 (272–440)	83	38,200 (3,160–73,240)	6,475

[a] Values in parentheses are 95% confidence intervals.
[b] Increases are calculated relative to *PMS1*.

An *ogg1*Δ allele was introduced into the *PMS1*, *pms1*Δ, *pms1-G882E*, and *pms1-H888R* strains containing the *LYS2F-10C* allele or the *LYS2R-10C* allele, in which GO lesions should be present within the leading- or lagging-strand template run, respectively (see Fig. 4). In each *ogg1* mutant, the rate of frameshifts in the 10G/10C run was increased at least fivefold relative to the rate in the corresponding *OGG1* parent strain (Table 5). In either the *PMS1 ogg1* or the *pms1*Δ *ogg1* strain, the rate of slippage within the 10G/10C run was same regardless of whether the G run was on the leading- or the lagging-strand template. Therefore, at least in the case of the *LYS2-10C* alleles used here, there appears to be neither a strand-related difference in the rate of polymerase slippage within G/C runs nor a strand-specific bias in the efficiency of MMR. In addition, the very strong bias for the accumulation of +1 frameshifts was evident in the *pms1-G882E ogg1* and the *pms1-H888R ogg1* strains, regardless of whether the 10G run was on the leading- or lagging-strand template. We estimate that the repair efficiencies of template strand loops in these strains was >90%, while that of primer strand loops was less than 1%. These data confirm that the novel *pms1* alleles reported here are specifically defective in the repair of primer strand loops generated during leading- and lagging-strand DNA replication.

***pms1-G882E* and *pms1-H888R* impact MMR and synergize with the +1-bp frameshift mutator allele, *pol2-C1089Y*.** Previously, a mutation in DNA polymerase ε, *pol2-C1089Y*, was reported to elevate preferentially +1-bp frameshift mutations within mononucleotide runs in yeast (33). As expected for a DNA polymerase defect, *pol2-C1089Y* synergized with *msh2*Δ for +1-bp frameshifts in mononucleotide runs (33). To address whether the *pms1-G882E* and *pms1-H888R* strains indeed reflect defects in MMR rather than some aspect of replication per se, we constructed double mutant strains containing *pms1* alleles together with either *msh2*Δ or *pol2-C1089Y*. As shown in Table 6, *pms1*Δ, *pms1-G882E*, and *pms1-H888R* mutations displayed epistatic interactions with *msh2*Δ, most relevantly for the *his7-2* +1-bp frameshift assay. In contrast, all three *pms1* alleles showed synergistic interactions with *pol2-C1089Y* in both the *CAN1* forward and *his7-2* reversion assays. Furthermore, *pol2-C1089Y* did not synergize with *pms1-G882E* or *pms1-H888R* using the −1-bp frameshift specific reporter, *hom3-10* (data not shown). These results strongly suggest that both *pms1-G882E* and *pms1-H888R* alleles specifically impact mismatch repair of +1-nucleotide primer-strand loops.

***pms1-G882E* and *pms1-H888R* efficiently repair 1-nucleotide loop mispairs during meiotic recombination.** In addition to a mitotic mutation avoidance role, MMR proteins also function during meiotic recombination. During recombination, sequence nonidentities between recombining alleles can result in mismatches in heteroduplex DNA intermediates (47, 52). Such mismatches are normally subject to mismatch correction, which can lead to gene conversion. However, failure of MMR will result in two nonidentical daughter cells when persisting heteroduplex DNA is replicated, which is termed postmeiotic segregation (PMS). Hence in wild-type cells, efficient heteroduplex repair will result in relatively high levels of gene conversion and low levels of PMS. In contrast, MMR-deficient strains will display increased levels of PMS at the expense of gene conversion events.

To determine the effect of *pms1-G882E* and *pms1-H888R* on the correction of 1-nucleotide loop mispairs in meiotic heteroduplex DNA, we used the haploid backgrounds AS4 and PD24. The resultant diploids are identical in sequence for the *HIS4* locus, except for being heterozygous for *his4-713*, a 1-bp insertion near the C terminus of *HIS4*. Furthermore, these diploids show high levels of non-Mendelian (aberrant) segregation initiated by double-strand breaks in the *HIS4* promoter region (11, 15). As shown in Table 7, the overall percentage of aberrant segregants, i.e., 6:2 plus 5:3, was similar in all diploid strains tested (20 to 30%). In wild type, *pms1-G882E* and *pms1-H888R* diploids, high levels of gene conversion, i.e., 6:2, and a low levels of PMS, i.e., 5:3, were observed, indicating efficient MMR of the 1-nucleotide loop mispair at *his4-713* (Table 7). Given that the two *HIS4* chromosomes used in the diploids strains experience double-strand breaks with identical frequencies (J. L. Arqueso and T. D. Petes, personal communication), the observed equal ratios of 6:2 versus 2:6 tetrads in the *PMS1*, *pms1-G882E*, and *pms1-H888R* strains suggest that there is no bias in the repair of the 1-nucleotide loop heteroduplex. As expected for MMR deficiency, *pms1*Δ diploids displayed significantly increased levels of PMS and reduced levels

TABLE 7. Meiotic mismatch repair of a 1-nucleotide loop heteroduplex at *HIS4*[a]

Strain	Total no. of tetrads	No. of tetrads					No. of other AB tetrads	% AB tetrads	% PMS/AB tetrads	Relative increase in PMS
		$4^+:4^-$	$6^+:2^-$	$2^-:6^+$	$5^+:3^-$	$3^+:5^-$				
PMS1	198	158	16	22	1	1	0	20	5	1
*pms1*Δ	66	46	2	5	4	7	2	30	55	11
pms1-G882E	203	159	12	23	2	2	5	22	9	1.8
pms1-H888R	197	145	15	27	3	4	3	26	13	2.4

[a] AB, aberrant.

of gene conversion. (Table 7, 45% gene conversion and 55% PMS). Whereas differences between PMS levels in the *pms1*Δ mutant and the wild type ($P < 0.0001$), *pms1-G882E* ($P = 0.0001$), and *pms1-H888R* ($P = 0.0003$) are highly significant, the differences in PMS levels between wild type and *pms1-G882E* and *pms1-H888R* were not significant (data not shown). Thus, these results indicate that neither *pms1-G882E* nor *pms1-H888R* significantly alters the repair efficiency of 1-nucleotide loop mismatches in heteroduplex DNA during meiotic recombination.

DISCUSSION

To understand better the function of MutLα during MMR-mediated mutation avoidance, we screened for alleles of *PMS1* that exhibit novel effects on mutational spectra. We identified two alleles, *pms1-G882E* and *pms1-H888R*, that greatly elevated the rate of +1-bp frameshifts in mononucleotide runs, while having relatively little effect on the rates of −1-bp frameshifts or base substitutions. The repair bias initially was observed in the *hom3-10* and *his7-2* frameshift reversion assays, which report −1-bp and +1-bp frameshifts in A/T runs, respectively, as well as in forward mutation spectra at *CAN1* (Tables 3 and 4). The generality of the strikingly inefficient repair of +1 frameshift intermediates was confirmed using a novel assay (Fig. 4), which determined mutational rates and spectra for C/G mononucleotide runs during leading- versus lagging- strand replication (Table 5). Using this assay, we showed that the *pms1-G882E* and *pms1-H888R* alleles were predominantly defective in the repair of primer strand loops generated during both leading- and lagging-strand DNA replication. Finally, the observed efficient repair of 1-nucleotide loops in meiotic heteroduplex DNA intermediates in *pms1-G882E* and *pms1-H888R* mutants (Table 6) suggests that the repair bias for primer strand versus template strand loops is related to mismatch repair that occurs in the context of DNA replication and not meiotic recombination. Interestingly, the mutations in the *pms1-G882E* and *pms1-H888R* alleles are in close proximity, affecting the COOH-terminus of Pms1 in a previously uncharacterized but highly conserved sequence motif.

Frameshift intermediates in repeat tracts are generated during DNA synthesis when the template and primer strands dissociate transiently and then reanneal in a misaligned configuration, resulting in single-strand loops of one or more repeats. If left unrepaired, 1-nucleotide loop mispairs will give rise, in the next round of replication, to 1-bp insertions or deletions, depending on whether the extra nucleotides are in the primer or the template strand, respectively (Fig. 3). While DNA polymerase generates comparable numbers of misaligned nucleotides on the template and primer strands when replicating simple sequence repeats, the MMR system appears to be inherently more efficient at repairing template strand loops than primer strand loops (21, 64, 68). One explanation for the more efficient repair of template strand loops in wild-type strains is that the MutS complexes differentially recognize primer strand versus template strand loops. The results reported here with *pms1-G882E* and *pms1-H888R* alleles suggest, however, that this inherent inefficiency of MMR is not a MutS recognition issue but, rather, reflects a processing difference dependent on Pms1 and, likely, Mlh1.

Although mutations in *PMS1* most likely affect the repair and not the generation of mutational intermediates, we asked first whether the *pms1-G882E* or *pms1-H888R* mutations impact MMR, per se, and then whether they might in some manner alter the polymerization fidelity through mononucleotide repeats. To address these questions, we performed epistasis analysis between *pms1* mutations and *msh2*Δ, as well as the DNA polymerase ε allele, *pol2-C19089Y*, which preferentially elevates +1-bp frameshifts in monoucleotide runs. We found that the *pms1*Δ, *pms1-G882E*, and *pms1-H888R* alleles all displayed epistatic interactions with *msh2*Δ. As observed previously (33), when combined with a *msh2*Δ allele, *pol2-C1089Y* synergized with *pms1*Δ for + 1-bp frameshifts in mononucleotide runs (Table 6). In contrast to the epistatic relationship with *msh2*Δ, *pms1-G884E* and *pms1-H888R* both synergized with the *pol2-C1089Y* for +1-bp frameshifts in the *his7-2* assay (Table 6). These results strongly suggest that *pms1-G882E* and *pms1-H888R* indeed impact mismatch repair of 1-nucleotide primer strand loops rather than affecting some aspect of the actual replication process.

To gain further understanding into the defects of *pms1-G882E* and *pms1-H888R*, we investigated the frameshifts generated in C/G runs during leading- versus lagging-strand synthesis. In yeast, previous studies exploiting the *OGG1* deficiency to assign the strand on which mutations arise suggested that mismatch repair of base/base mispairs was more efficient during lagging-strand than leading-strand replication (51). We addressed this issue for frameshifts in mononucleotide runs by a similar approach and incorporated *ogg1*Δ into strains containing the G/C run *LYS2* reporter located near an origin of replication (Fig. 4). In these strains, the G run was present on either the leading- or lagging-strand template during replication. *ogg1*Δ increased frameshifts in the runs and therefore allowed the marking of the template that contained the GO lesion. In addition, *ogg1*Δ displayed synergistic interactions with *pms1*Δ, *pms1-G882E*, and *pms1-H888R* (Table 5),

suggesting increased polymerase slippage due to unrepaired GO lesions. Importantly, whereas most mutations in the *pms1*Δ *ogg1*Δ strains were −1 frameshifts, more than 95% of the frameshifts in the *pms1-G882E ogg1*Δ and *pms1-H888R ogg1*Δ were +1 frameshifts. Taken together, these data indicate that both *pms1* alleles primarily affect repair of primer strand loops during both leading- and lagging-strand synthesis. In turn, these findings are consistent with the current view for association between MMR and replication machinery (28, 31, 69).

Further insight into the defect of the *pms1-G884E* and *pms1-H888R* mutants emerged from examining the effects of these alleles on heteroduplex correction during meiotic recombination. Relative to a *pms1*Δ strain, both mutant strains efficiently repaired meiotic heteroduplexes containing 1-nucleotide loops (Table 7). This implies that there is a difference between the processing of replication- and recombination-associated mispairs in these mutants. Although there are many factors that may contribute to this difference, we suggest that the recognition of loop mispairs during meiotic recombination is likely to be independent of the DNA synthesis machinery, whereas MMR-mediated mutation avoidance is linked to replication (4, 9, 18, 22, 34, 36, 51, 69).

The *pms1-G882E* and *pms1-H888* mutations that cause the preferential elevation of +1-bp frameshifts in mononucleotide runs map in the C-terminal 200 amino acids of Pms1 to a 13-amino-acid motif that is highly conserved in eukaryotic Pms1 homologs. Because the C-terminal region of Pms1 is required for interaction with Mlh1 (49), the novel mutator phenotypes might simply reflect abnormal MutLα heterodimer formation. However, the *pms1-G882E* and *pms1-H888* mutations had no detectable effect on Pms1 stability or interaction with Mlh1 as determined with the two-hybrid assay. The C-terminal domain of MutL has been shown to be important for homodimerization (1, 12), interactions with MutH and UvrD (25, 26), and DNA binding (27). Furthermore, based on the recently solved crystal structure of the COOH-terminus of MutL (23), the residues affected by the *pms1* alleles studied here appear to be in an exposed region of the protein and, therefore, may be important for interaction with other proteins and/or DNA during MMR. Further studies of these *pms1* alleles and other mutations with specific mutator effects should shed additional light on eukaryotic MMR, possibly including the mechanism of strand discrimination.

ACKNOWLEDGMENTS

We thank Gray Crouse, Rodney Rothstein, Marcel Wehrli, Jennifer Johnson, and Ashleigh Miller, for critical reading of the manuscript.

This work was supported by National Institutes of Health (NIH) grant 5 R0l GM45413 to R.M.L. and NIH grant GM038464 to S.J.R.; N.E. was supported by NIH fellowship F32 GM20342, and R.G. was partially supported by the Graduate Division of Biological and Biomedical Sciences at Emory University.

REFERENCES

1. **Ban, C., and W. Yang.** 1998. Crystal structure and ATPase activity of MutL: implications for DNA repair and mutagenesis. Cell **95:**541–552.
2. **Baudin, A., O. Ozier-Kalogeropoulos, A. Denouel, F. Lacroute, and C. Cullin.** 1993. A simple and efficient method for direct gene deletion in *Saccharomyces cerevisiae*. Nucleic Acids Res. **21:**3329–3330.
3. **Bellacosa, A.** 2001. Functional interactions and signaling properties of mammalian DNA mismatch repair proteins. Cell Death Differ. **8:**1076–1092.
4. **Bowers, J., P. T. Tran, A. Joshi, R. M. Liskay, and E. Alani.** 2001. MSH-MLH complexes formed at a DNA mismatch are disrupted by the PCNA sliding clamp. J. Mol. Biol. **306:**957–968.
5. **Bronner, C. E., S. M. Baker, P. T. Morrison, G. Warren, L. G. Smith, M. K. Lescoe, M. Kane, C. Earabino, J. Lipford, A. Lindblom, P. Tannergard, R. J. Bollag, A. R. Godwin, D. C. Ward, M. Nordenskjold, R. Fishel, R. Kolodner, and R. M. Liskay.** 1994. Mutation in the DNA mismatch repair gene homologue *hMLH1* is associated with hereditary nonpolyposis colon cancer. Nature **368:**258–261.
6. **Brown, K. D., A. Rathi, R. Kamath, D. I. Beardsley, Q. Zhan, J. L. Mannino, and R. Baskaran.** 2003. The mismatch repair system is required for S-phase checkpoint activation. Nat. Genet. **33:**80–84.
7. **Buermeyer, A. B., S. M. Deschenes, S. M. Baker, and R. M. Liskay.** 1999. Mammalian DNA mismatch repair. Annu. Rev. Genet. **33:**533–564.
8. **Chattoo, B. B., F. Sherman, T. A. Azubalis, T. A. Fjellstedt, D. Mehnert, and M. Ogur.** 1979. Selection of *lys2* mutants of yeast *Saccharomyces cerevisiae* by the utilization of α-aminoadipate. Genetics **93:**51–65.
9. **Clark, A. B., F. Valle, K. Drotschmann, R. K. Gary, and T. A. Kunkel.** 2000. Functional interaction of proliferating cell nuclear antigen with MSH2-MSH6 and MSH2-MSH3 complexes. J. Biol. Chem. **275:**36498–36501.
10. **Dao, V., and P. Modrich.** 1998. Mismatch-, MutS-, MutL-, and helicase II-dependent unwinding from the single-strand break of an incised heteroduplex. J. Biol. Chem. **273:**9202–9207.
11. **Detloff, P., M. A. White, and T. D. Petes.** 1992. Analysis of a gene conversion gradient at the *HIS4* locus in *Saccharomyces cerevisiae*. Genetics **132:**113–123.
12. **Drotschmann, K., A. Aronshtam, H. J. Fritz, and M. G. Marinus.** 1998. The *Escherichia coli* MutL protein stimulates binding of Vsr and MutS to heteroduplex DNA. Nucleic Acids Res. **26:**948–953.
13. **Edelmann, L., and W. Edelmann.** 2004. Loss of DNA mismatch repair function and cancer predisposition in the mouse: animal models for human hereditary nonpolyposis colorectal cancer. Am. J. Med. Genet. C **129:**91–99.
14. **Erdeniz, N., U. H. Mortensen, and R. Rothstein.** 1997. Cloning-free PCR-based allele replacement methods. Genome Res. **7:**1174–1183.
15. **Fan, Q., F. Xu, and T. D. Petes.** 1995. Meiosis-specific double-strand DNA breaks at the *HIS4* recombination hot spot in the yeast *Saccharomyces cerevisiae*: control in *cis* and *trans*. Mol. Cell. Biol. **15:**1679–1688.
16. **Fishel, R., M. K. Lescoe, M. R. Rao, N. G. Copeland, N. A. Jenkins, J. Garber, M. Kane, and R. Kolodner.** 1993. The human mutator gene homolog MSH2 and its association with hereditary nonpolyposis colon cancer. Cell **75:**1027–1038.
17. **Fleig, U. N., R. D. Pridmore, and P. Philippsen.** 1986. Construction of *LYS2* cartridges for use in genetic manipulations of *Saccharomyces cerevisiae*. Gene **46:**237–245.
18. **Flores-Rozas, H., D. Clark, and R. D. Kolodner.** 2000. Proliferating cell nuclear antigen and Msh2p-Msh6p interact to form an active mispair recognition complex. Nat. Genet. **26:**375–378.
19. **Flores-Rozas, H., and R. D. Kolodner.** 1998. The *Saccharomyces cerevisiae MLH3* gene functions in *MSH3*-dependent suppression of frameshift mutations. Proc. Natl. Acad. Sci. USA **95:**12404–12409.
20. **Goldstein, A. L., X. Pan, and J. H. McCusker.** 1999. Heterologous URA3MX cassettes for gene replacement in *Saccharomyces cerevisiae*. Yeast **15:**507–511.
21. **Gragg, H., B. D. Harfe, and S. Jinks-Robertson.** 2002. Base composition of mononucleotide runs affects DNA polymerase slippage and removal of frameshift intermediates by mismatch repair in *Saccharomyces cerevisiae*. Mol. Cell. Biol. **22:**8756–8762.
22. **Gu, L., Y. Hong, S. McCulloch, H. Watanabe, and G. M. Li.** 1998. ATP-dependent interaction of human mismatch repair proteins and dual role of PCNA in mismatch repair. Nucleic Acids Res. **26:**1173–1178.
23. **Guarne, A., S. Ramon-Maiques, E. M. Wolff, R. Ghirlando, X. Hu, J. H. Miller, and W. Yang.** 2004. Structure of the MutL C-terminal domain: a model of intact MutL and its roles in mismatch repair. EMBO J. **23:**4134–4145.
24. **Habraken, Y., P. Sung, L. Prakash, and S. Prakash.** 1997. Enhancement of *MSH2-MSH3*-mediated mismatch recognition by the yeast *MLH1-PMS1* complex. Curr. Biol. **7:**790–793.
25. **Hall, M. C., J. R. Jordan, and S. W. Matson.** 1998. Evidence for a physical interaction between the *Escherichia coli* methyl-directed mismatch repair proteins MutL and UvrD. EMBO J. **17:**1535–1541.
26. **Hall, M. C., and S. W. Matson.** 1999. The *Escherichia coli* MutL protein physically interacts with MutH and stimulates the MutH-associated endonuclease activity. J. Biol. Chem. **274:**1306–1312.
27. **Hall, M. C., P. V. Shcherbakova, J. M. Fortune, C. H. Borchers, J. M. Dial, K. B. Tomer, and T. A. Kunkel.** 2003. DNA binding by yeast Mlh1 and Pms1: implications for DNA mismatch repair. Nucleic Acids Res. **31:**2025–2034.
28. **Harfe, B. D., and S. Jinks-Robertson.** 2000. DNA mismatch repair and genetic instability. Annu. Rev. Genet. **34:**359–399.
29. **Harfe, B. D., and S. Jinks-Robertson.** 2000. Sequence composition and context effects on the generation and repair of frameshift intermediates in mononucleotide runs in *Saccharomyces cerevisiae*. Genetics **156:**571–578.
30. **Harfe, B. D., B. K. Minesinger, and S. Jinks-Robertson.** 2000. Discrete in

vivo roles for the MutL homologs Mlh2p and Mlh3p in the removal of frameshift intermediates in budding yeast. Curr. Biol. **10:**145–148.
31. **Jiricny, J.** 1998. Eukaryotic mismatch repair: an update. Mutat. Res. **409:** 107–121.
32. **Johnson, R. E., G. K. Kovvali, L. Prakash, and S. Prakash.** 1996. Requirement of the yeast *MSH3* and *MSH6* genes for *MSH2*-dependent genomic stability. J. Biol. Chem. **271:**7285–7288.
33. **Kirchner, J. M., H. Tran, and M. A. Resnick.** 2000. A DNA polymerase epsilon mutant that specifically causes +1 frameshift mutations within homonucleotide runs in yeast. Genetics **155:**1623–1632.
34. **Kleczkowska, H. E., G. Marra, T. Lettieri, and J. Jiricny.** 2001. hMSH3 and hMSH6 interact with PCNA and colocalize with it to replication foci. Genes Dev. **15:**724–736.
35. **Kolodner, R. D., and G. T. Marsischky.** 1999. Eukaryotic DNA mismatch repair. Curr. Opin. Genet. Dev. **9:**89–96.
36. **Lau, P. J., H. Flores-Rozas, and R. D. Kolodner.** 2002. Isolation and characterization of new proliferating cell nuclear antigen (*POL30*) mutator mutants that are defective in DNA mismatch repair. Mol. Cell. Biol. **22:**6669–6680.
37. **Lea, D., and C. Coulson.** 1948. The distribution of the number of mutants in bacterial populations. J. Genet. **49:**264–285.
38. **Leach, F. S., N. C. Nicolaides, N. Papadopoulos, B. Liu, J. Jen, R. Parsons, P. Peltomaki, P. Sistonen, L. A. Aaltonen, M. Nystrom-Lahti, X.-Y. Guan, J. Zhang, P. S. Meltzer, J.-W. Yu, F.-T. Kao, D. J. Chen, K. M. Cerosaletti, R. E. K. Fournier, S. Todd, T. Lewis, R. J. Leach, S. L. Naylor, J. Weissenbach, J.-P. Mecklin, H. Jarvinen, G. M. Petersen, S. R. Hamilton, J. Green, J. Jass, P. Watson, H. T. Lynch, J. M. Trent, A. de la Chapelle, K. W. Kinzler, and B. Vogelstein.** 1993. Mutations of a *mutS* homolog in hereditary nonpolyposis colorectal cancer. Cell **75:**1215–1225.
39. **Liang, Q., and T. Richardson.** 1992. A simple and rapid method for screening transformant yeast colonies using PCR. BioTechniques **13:**730–732, 735.
40. **Ma, H., S. Kunes, P. J. Schatz, and D. Botstein.** 1987. Plasmid construction by homologous recombination in yeast. Gene **58:**201–216.
41. **Marsischky, G. T., N. Filosi, M. F. Kane, and R. Kolodner.** 1996. Redundancy of *Saccharomyces cerevisiae MSH3* and *MSH6* in *MSH2*-dependent mismatch repair. Genes Dev. **10:**407–420.
42. **Marti, T. M., C. Kunz, and O. Fleck.** 2002. DNA mismatch repair and mutation avoidance pathways. J. Cell Physiol. **191:**28–41.
43. **Mechanic, L. E., B. A. Frankel, and S. W. Matson.** 2000. *Escherichia coli* MutL loads DNA helicase II onto DNA. J. Biol. Chem. **275:**38337–38346.
44. **Modrich, P., and R. Lahue.** 1996. Mismatch repair in replication fidelity, genetic recombination, and cancer biology. Annu. Rev. Biochem. **65:**101–133.
45. **New, L., K. Liu, and G. F. Crouse.** 1993. The yeast gene *MSH3* defines a new class of eukaryotic MutS homologues. Mol. Gen. Genet. **239:**97–108.
46. **Newlon, C. S., L. R. Lipchitz, I. Collins, A. Deshpande, R. J. Devenish, R. P. Green, H. L. Klein, T. G. Palzkill, R. B. Ren, S. Synn, et al.** 1991. Analysis of a circular derivative of *Saccharomyces cerevisiae* chromosome III: a physical map and identification and location of *ARS* elements. Genetics **129:**343–357.
47. **Nicolas, A., and T. D. Petes.** 1994. Polarity of meiotic gene conversion in fungi: contrasting views. Experientia **50:**242–252.
48. **Orr-Weaver, T. L., J. W. Szostak, and R. J. Rothstein.** 1983. Genetic applications of yeast transformation with linear and gapped plasmids. Methods Enzymol. **101:**228–245.
49. **Pang, Q., T. A. Prolla, and R. M. Liskay.** 1997. Functional domains of the *Saccharomyces cerevisiae* Mlh1p and Pms1p DNA mismatch repair proteins and their relevance to human hereditary nonpolyposis colorectal cancer-associated mutations. Mol. Cell. Biol. **17:**4465–4473.
50. **Papadopoulos, N., N. C. Nicolaides, Y.-F. Wei, S. M. Ruben, K. C. Carter, C. A. Rosen, W. A. Haseltine, R. D. Fleischmann, C. M. Fraser, M. D. Adams, J. C. Venter, S. R. Hamilton, G. M. Petersen, P. Watson, H. T. Lynch, P. Peltomaki, J.-P. Mecklin, A. de la Chapelle, K. W. Kinzler, and B. Vogelstein.** 1994. Mutation of a mutL homolog in hereditary colon cancer. Science **263:**1625–1629.
51. **Pavlov, Y. I., I. M. Mian, and T. A. Kunkel.** 2003. Evidence for preferential mismatch repair of lagging strand DNA replication errors in yeast. Curr. Biol. **13:**744–748.
52. **Petes, T. D.** 2001. Meiotic recombination hot spots and cold spots. Nat. Rev. Genet. **2:**360–369.
53. **Prolla, T. A., D. M. Christie, and R. M. Liskay.** 1994. Dual requirement in yeast DNA mismatch repair for *MLH1* and *PMS1*, two homologs of the bacterial *mutL* gene. Mol. Cell. Biol. **14:**407–415.
54. **Prolla, T. A., Q. Pang, E. Alani, R. D. Kolodner, and R. M. Liskay.** 1994. *MLH1*, *PMS1*, and *MSH2* interactions during the initiation of DNA mismatch repair in yeast. Science **265:**1091–1093.
55. **Scherer, S., and R. W. Davis.** 1979. Replacement of chromosome segments with altered DNA sequences constructed in vitro. Proc. Natl. Acad. Sci. USA **76:**4951–4955.
56. **Schofield, M. J., and P. Hsieh.** 2003. DNA mismatch repair: molecular mechanisms and biological function. Annu. Rev. Microbiol. **57:**579–608.
57. **Shcherbakova, P. V., and T. A. Kunkel.** 1999. Mutator phenotypes conferred by *MLH1* overexpression and by heterozygosity for *mlh1* mutations. Mol. Cell. Biol. **19:**3177–3183.
58. **Sherman, F.** 1991. Getting started with yeast. Methods Enzymol. **194:**3–21.
59. **Sia, E. A., R. J. Kokoska, M. Dominska, P. Greenwell, and T. D. Petes.** 1997. Microsatellite instability in yeast: dependence on repeat unit size and DNA mismatch repair genes. Mol. Cell. Biol. **17:**2851–2858.
60. **Sikorski, R. S., and P. Hieter.** 1989. A system of shuttle vectors and yeast host strains designed for efficient manipulation of DNA in *Saccharomyces cerevisiae*. Genetics **122:**19–27.
61. **Stapleton, A., and T. D. Petes.** 1991. The Tn3 beta-lactamase gene acts as a hotspot for meiotic recombination in yeast. Genetics **127:**39–51.
62. **Stojic, L., R. Brun, and J. Jiricny.** 2004. Mismatch repair and DNA damage signalling. DNA Repair **3:**1091–1101.
63. **Storici, F., L. K. Lewis, and M. A. Resnick.** 2001. *In vivo* site-directed mutagenesis using oligonucleotides. Nat. Biotechnol. **19:**773–776.
64. **Strand, M., M. C. Earley, G. F. Crouse, and T. D. Petes.** 1995. Mutations in the *MSH3* gene preferentially lead to deletions within tracts of simple repetitive DNA in *Saccharomyces cerevisiae*. Proc. Natl. Acad. Sci. USA **92:** 10418–10421.
65. **Thomas, B. J., and R. Rothstein.** 1989. Elevated recombination rates in transcriptionally active DNA. Cell **56:**619–630.
66. **Tran, H. T., J. D. Keen, M. Kricker, M. A. Resnick, and D. A. Gordenin.** 1997. Hypermutability of homonucleotide runs in mismatch repair and DNA polymerase proofreading yeast mutants. Mol. Cell. Biol. **17:**2859–2865.
67. **Tran, P. T., and R. M. Liskay.** 2000. Functional studies on the candidate ATPase domains of *Saccharomyces cerevisiae* MutLα. Mol. Cell. Biol. **20:** 6390–6398.
68. **Twerdi, C. D., J. C. Boyer, and R. A. Farber.** 1999. Relative rates of insertion and deletion mutations in a microsatellite sequence in cultured cells. Proc. Natl. Acad. Sci. USA **96:**2875–2879.
69. **Umar, A., A. B. Buermeyer, J. A. Simon, D. C. Thomas, A. B. Clark, R. M. Liskay, and T. A. Kunkel.** 1996. Requirement for PCNA in DNA mismatch repair at a step preceding DNA resynthesis. Cell **87:**65–73.
70. **van der Kemp, P. A., D. Thomas, R. Barbey, R. de Oliveira, and S. Boiteux.** 1996. Cloning and expression in *Escherichia coli* of the *OGG1* gene of *Saccharomyces cerevisiae*, which codes for a DNA glycosylase that excises 7,8-dihydro-8-oxoguanine and 2,6-diamino-4-hydroxy-5-*N*-methylformamidopyrimidine. Proc. Natl. Acad. Sci. USA **93:**5197–5202.
71. **von Borstel, R. C., E. A. Savage, Q. Wang, U. G. Hennig, R. G. Ritzel, G. S. Lee, M. D. Hamilton, M. A. Chrenek, R. W. Tomaszewski, J. A. Higgins, C. J. Tenove, L. Liviero, P. J. Hastings, C. T. Korch, and C. M. Steinberg.** 1998. Topical reversion at the *HIS1* locus of *Saccharomyces cerevisiae*. A tale of three mutants. Genetics **148:**1647–1654.
72. **Wang, T. F., N. Kleckner, and N. Hunter.** 1999. Functional specificity of MutL homologs in yeast: evidence for three Mlh1-based heterocomplexes with distinct roles during meiosis in recombination and mismatch correction. Proc. Natl. Acad. Sci. USA **96:**13914–13919.
73. **Welz-Voegele, C., J. E. Stone, P. T. Tran, H. M. Kearney, R. M. Liskay, T. D. Petes, and S. Jinks-Robertson.** 2002. Alleles of the yeast *PMS1* mismatch-repair gene that differentially affect recombination- and replication-related processes. Genetics **162:**1131–1145.
74. **Yamaguchi, M., V. Dao, and P. Modrich.** 1998. MutS and MutL activate DNA helicase II in a mismatch-dependent manner. J. Biol. Chem. **273:**9197–9201.
75. **Zhao, X., B. Georgieva, A. Chabes, V. Domkin, J. H. Ippel, J. Schleucher, S. Wijmenga, L. Thelander, and R. Rothstein.** 2000. Mutational and structural analyses of the ribonucleotide reductase inhibitor Sml1 define its Rnr1 interaction domain whose inactivation allows suppression of *mec1* and *rad53* lethality. Mol. Cell. Biol. **20:**9076–9083.
76. **Zhu, J., C. S. Newlon, and J. A. Huberman.** 1992. Localization of a DNA replication origin and termination zone on chromosome III of *Saccharomyces cerevisiae*. Mol. Cell. Biol. **12:**4733–4741.
77. **Zou, H., and R. Rothstein.** 1997. Holliday junctions accumulate in replication mutants via a RecA homolog-independent mechanism. Cell **90:**87–96.